

UNVEILING THE BOXY BULGE AND BAR OF THE ANDROMEDA SPIRAL GALAXY

RACHAEL L. BEATON¹, STEVEN R. MAJEWSKI¹, PURAGRA GUHATHAKURTA², MICHAEL F. SKRUTSKIE¹,
 ROC M. CUTRI³, JOHN GOOD³, RICHARD J. PATTERSON¹, E. ATHANASSOULA⁴, AND MARTIN BUREAU⁴

Draft version September 3, 2018

ABSTRACT

A new, 2.8 deg² J, H, K_s infrared survey from the 2MASS 6x program across the extent of the optical disk of the Andromeda (M31) galaxy provides a clear view of the M31 center almost completely unfettered by dust extinction, and reveals a high contrast bulge with extremely boxy isophotes dominating the NIR light to a semi-major axis of $\sim 700''$ (2.6 kpc). The inner bulge ($\lesssim 50''$) is relatively circular, but shows some isophotal twisting. Beyond this, the ellipticity and boxiness of the bulge increase with radius — achieving a boxiness that rivals that of any other known disk galaxy observed in the near infrared — and the position angle is constant at $\sim 50^\circ$, which is about 10° higher than the position angle of the M31 disk. Boxy bulges in highly inclined disks have been shown to be the vertical structure of bars, and self-consistent, N -body modeling specific to the NIR images presented here can reproduce the observed NIR M31 features with a combination of a classical bulge and a boxy bulge/bar. Beyond the boxy bulge region and nearly along the 40° position angle of the disk a narrow ridge of infrared flux, which can be identified with the thin part of the bar, more or less symmetrically extends into the inner disk at semi-major axis radii of $700''$ to $1200''$ or more. Little variation in the morphology or relative brightnesses of these various M31 structures is seen across the NIR bands (i.e., no color gradients are seen). These new data verify that M31 is a barred spiral galaxy like the Milky Way.

Subject headings: galaxies: individual (M31); Local Group; Galactic Bulges; Infrared Photometry; Galaxies (bars)

1. INTRODUCTION

For long after the discovery that spiral nebulae are “island universes”, the Andromeda Galaxy (M31) was thought to present a reasonable mirror image of our own Milky Way. This morphological mirror, however, was clouded with the discovery of barred structure in the Milky Way, revealed both as a gas dynamical structure (Blitz et al. 1993) and a stellar feature (Weinberg 1992). More recent evidence (e.g., Parker et al. 2003, 2004; see also Newberg & Yanny 2004) suggests that the Milky Way’s central bar may exert significant influence, or at least account for observable stellar density asymmetries, to large distances from the Galactic mid-plane.

Although there have been isolated lines of evidence supporting the existence of a bar in M31, its existence has remained uncertain. Fifty years ago Lindblad (1956) first recognized a general misalignment of the innermost isophotes of M31 with the major axis of the outer isophotes. This was interpreted as an indication that the bulge was triaxial due to the presence of a nuclear bar. Stark (1977) attempted to match the observed isophotal twists and overall optical surface brightness

distribution within 2 kpc with a one-parameter family of triaxial models, and also concluded that misalignment between the bulge and disk isophotes required a central bar. This notion was supported by evidence from gas dynamics (Stark & Binney 1994, Berman 2001; Berman & Loinard 2002). Kinematical work in the nucleus of M31 (Kormendy 1988; Dressler & Richstone 1988) revealed large rotation velocities, initially interpreted as evidence of a supermassive black hole at the center of M31, but later explained using bar-like potentials (Gerhard 1988). Though Kent’s (1983) optical imaging did not identify the previously suggested misalignment of the bulge and disk isophotes, the data showed some degree of boxiness to the bulge isophotes, revealed by a non-zero fourth-order harmonic in observed isophotal shapes. The boxy classification of M31’s bulge by Kent (1983) makes a compelling implication of a more complicated central M31. However, all previous optical studies of M31 have been substantially hindered by dust contamination in this highly inclined ($i = 77.5^\circ$) system.

It has long been known that observations in the near-infrared (NIR), where the effects of dust are mitigated, can reveal central galaxy structures hidden at shorter wavelengths, including multiple nuclei, bars, and boxy/peanut-shaped bulges (e.g., Hackwell & Schweizer 1983, Scoville et al. 1988, Telesco et al. 1991, Majewski et al. 1993, Quillen et al. 1997). The central regions of highly inclined systems are particularly challenging, but especially valuable for understanding the frequency of boxy/peanut morphologies. Despite several surveys of highly-inclined galaxies (e.g., Shaw 1993, Lütticke et al. 2000, Bureau et al. 2006), perhaps less than 100 have been studied in the NIR. This includes the Milky Way, for which a clear portrait of its central, bar-like structure

¹ Department of Astronomy, University of Virginia, Charlottesville, Virginia 22903-0818; rlb9n@virginia.edu, srm4n@virginia.edu, mfs4n@virginia.edu, rjp0i@virginia.edu

² UCO/Lick Observatory, Department of Astronomy & Astrophysics, University of California, Santa Cruz, California 95064; raja@ucolick.org

³ Infrared Processing and Analysis Center, Caltech, MS 100-22, Pasadena, CA 91125; roc@ipac.caltech.edu, jeg@ipac.caltech.edu

⁴ Observatoire de Marseille, 2 place Le Verrier, 13248 Marseille Cedex 04, France; lia@oamp.fr

⁵ Sub-Department of Astrophysics, University of Oxford, Denys Wilkinson Building, Keble Road, Oxford OX1 3RH, United Kingdom; bureau@astro.ox.ac.uk

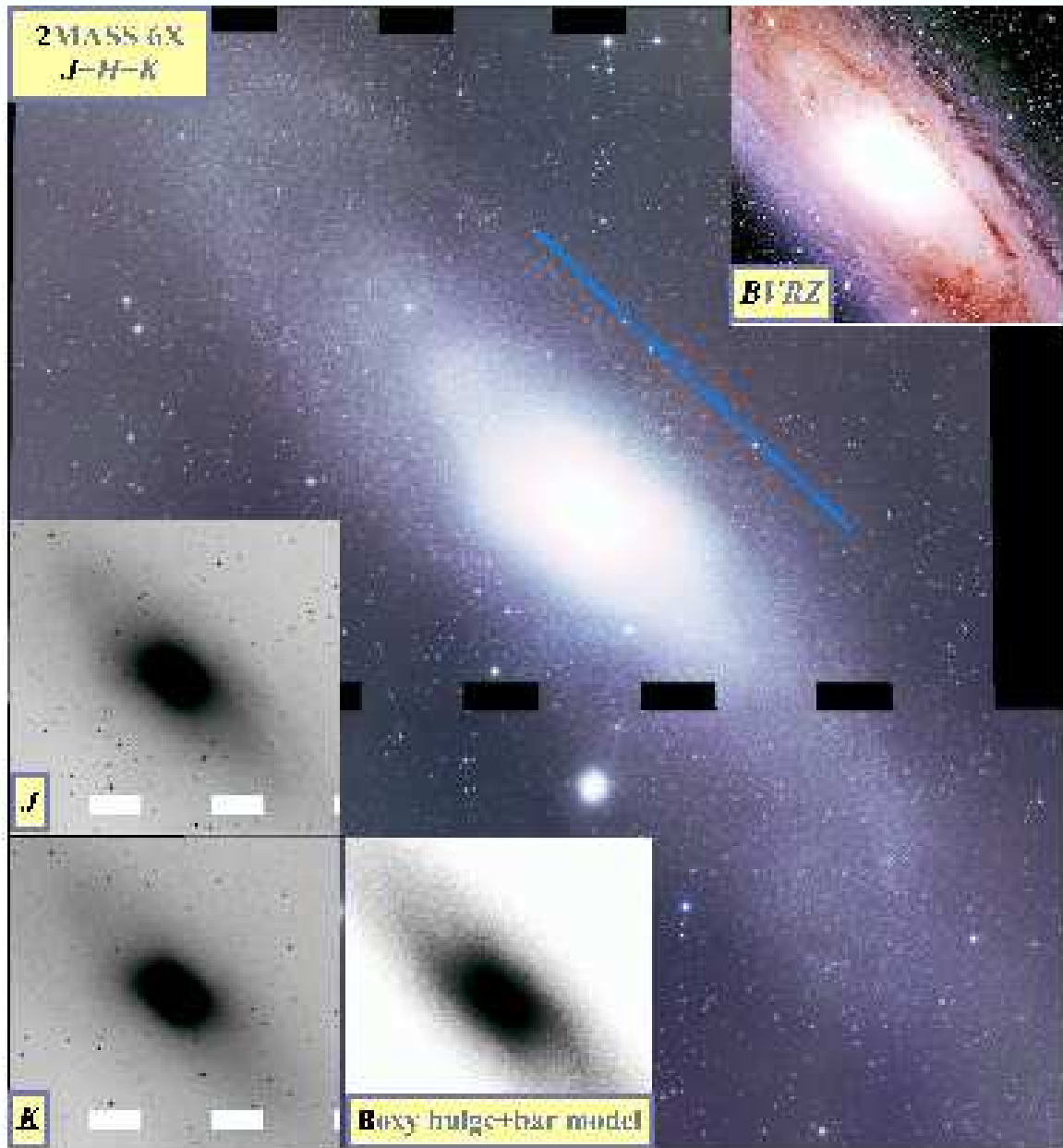


FIG. 1.— The central image is a color composite using the J, H, K_s images of M31 from the 2MASS 6x observations. The line is $40'$ (8kpc) long. Two of these contributing images (J and K_s) are shown in the lower left insets. The upper right inset is a color composite from the optical B, V, R, z bands. An additional inset shows a boxy bulge plus bar model matching the system from Athanassoula & Beaton (2006). Insets are 30% smaller than the central image.

has been revealed by the distribution of carbon stars in the Two Micron All Sky Survey (2MASS) point source catalog (Skrutskie et al. 2001, Cole & Weinberg 2002). Comparable studies of M31 have not been previously available because of the combined need for greater depth over a large field of view. Such a view is now provided by deep scans of M31 using the 2MASS North facility.

2. THE 6X OBSERVATIONS OF M31

Near the end of the normal 2MASS observing period, long exposure observations were taken of a number of special target regions, including M31, during idle times in the regular operation of the survey. These observations,

taken with exposures six times longer than the nominal 2MASS observations and referred to as the “6x observations”, used the same freeze-frame scanning as the main survey.⁶ M31 was observed using 1° long scans similar to those used for 2MASS calibration field observations. A telescope command error produced coverage gaps of a few arcmin² in the 2.8 deg^2 M31 6x mosaic. These gaps (visible in Fig. 1) do not affect the work presented here.

We adopt the standard reduction of the 6x M31 data provided by the 2MASS Project, which used a

⁶ See <http://www.ipac.caltech.edu/2mass/releases/allsky/doc/> for a description of the 2MASS 6x survey.

slightly modified version of the automated data reduction pipeline utilized to process the original survey data. The final output 6x Atlas Images are identical in format to those from the original survey. Composite J , H and K_s mosaics were constructed from the individual 6x M31 Atlas Images using the Montage⁷ software package. Montage matches the background levels of all images by applying an additive offset and gradient correction that is computed using a least-squares fit to the mean intensity offsets of all pixels in the overlapping regions between each pair of images. No correction was applied to the images to match the photometric zero points between adjacent 6x scans. However, the relative zero points variation is $< 1\%$ in all bands over the region of the M31 bulge, so there should be no discernable effect on the surface brightness fits. From these mosaics, a mean “sky” level was determined from the peak of the histogram of pixel values in the outer image, beyond the apparent disk of M31, which is defined by the ring of HII regions readily apparent in the GALEX images of M31 (e.g., see Thilker et al. 2005). This offset value determined for each J , H and K_s image was subtracted to adjust pixel values to an approximately linear representation of M31 flux; this is sufficient for our present goal to understand the overall morphology of the M31 center.

3. THE NEAR-INFRARED STRUCTURE OF M31

A boxy, high surface brightness central bulge is the most obvious M31 feature in the 6x images, and this significantly distinguishes M31’s NIR morphology from that seen in the optical (Fig. 1). Apart from slightly more dust modulation in J , the basic character of M31 system is the same across the NIR bands, most evidently in the similarity of the high contrast region of the bulge with its $\sim 700''$ major axis radius and, at fainter surface brightness, the appearance of a thin ridge of NIR light just beyond this bulge nearly along the disk major axis.

To quantify this morphology, ellipses were fit to the isophotal contours in each the J , H and K_s bands using the ELLIPSE package in IRAF (Fig. 2). This code uses the techniques of Jedrzejewski (1987) to fit a Fourier series to concentric galactic isophotes. The fourth order coefficients (A_4 and B_4) of the best fit Fourier series are a useful descriptor of the deviation of the isophotes from true ellipses, from “boxy” ($B_4 < 0$, $A_4 > 0$) to “disky” ($B_4 > 0$, $A_4 < 0$). The strong boxiness of the M31 bulge is evident not only by its Fourier decomposition (Fig. 3) but by the difference between the galaxy isophotes and their corresponding best-fitting ellipses (Fig. 2). The ELLIPSE algorithm also determines the position angle (PA) of the major axis of each isophote and its ellipticity ($e = 1 - b/a$); these are shown in Figure 3. We discuss the full NIR M31 surface brightness profile derived from the 6x data, and its bulge/disk decomposition, elsewhere.

Based on trends in Figures 2–3, we discriminate four observational regions by semimajor axis radius within the inner $\sim 3300''$ of M31 (see divisions in Fig. 3): (1) A moderately circular nucleus dominates the central $< 3''$. The nucleus was shown to be an independent feature of M31 (Light et al. 1974), so the characteristics within $3''$ do not bear on the morphology of the bulge. In any case, because of the $1''$ pixel sampling, the PA and Fourier de-

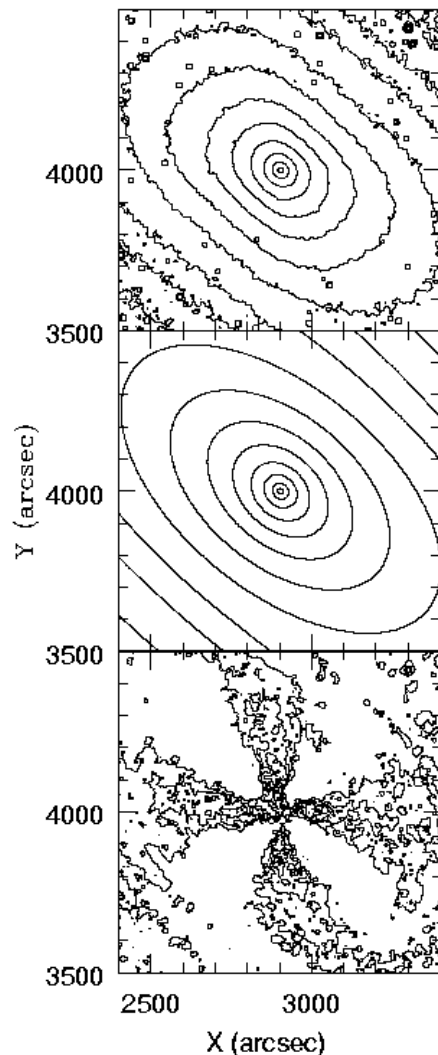


FIG. 2.— *Top*: Contour plot for the central K_s band image. *Middle*: Best fit ellipses to the K_s data. *Bottom*: Residual plots created by subtracting the best fitting ellipse from the K_s data. The contours in all three panels have uniform logarithmic spacing. The pixel coordinates are pixel values in the 6x image; the image scale is $1''$ pixel $^{-1}$. The X and Y coordinates are aligned with the right ascension and declination axes.

composition here have little meaning. (2) A near-circular bulge ($3''$ to $50''$) resembling a classical bulge with low ellipticity and some diskiness. The primary structural characteristic of this radial zone is a 20° change in position angle. This isophotal twisting is evident by the slight kinking of the innermost parts of the “Maltese cross” pattern in the bottom panel of Figure 2. (3) The boxy bulge ($\sim 50''$ to $\sim 700''$) exhibits distinctly negative values of B_4/B and a steadily increasing ellipticity with radius (at constant PA). The strongest boxiness, at $\sim 300''$, is evident by the width and amplitude of the Maltese cross arms at this point. Finally, (4) a transition to the inner disk ($> 700''$) is demarcated by the shift to diskier Fourier components and by the lower surface brightness evident in Figure 1. Because of the lower surface brightness and partial coverage, the PA and ellipticity are less reliably measured here. However, an obvious feature in this radial zone is the narrow bar structure protruding from both ends of the boxy bulge, shifted to nearly the

⁷ See <http://montage.ipac.caltech.edu/>.

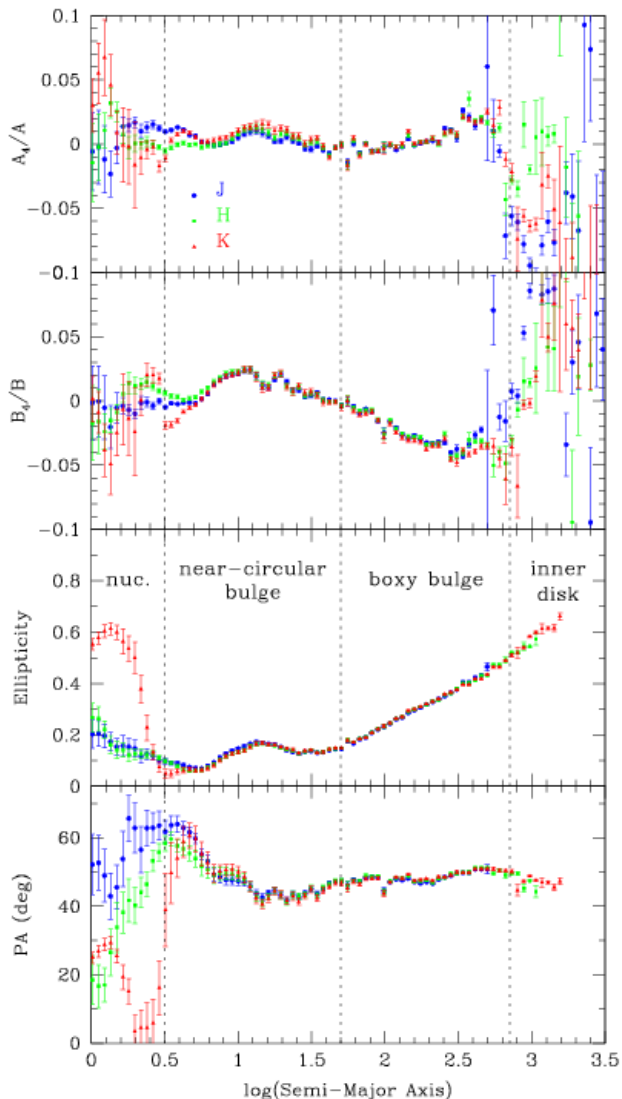


FIG. 3.— A_4/A , B_4/B , ellipticity and position angle of M31 as a function of semi-major axis (in arcseconds) as measured in the J , H and K_s bands (blue, green and red points, respectively).

disk PA, and extending to a radius of $\sim 1200''$ (4 kpc) or more.

Several trends hold throughout the bulge/bar regions just described: (a) The three infrared bands closely track one another in morphology and relative brightness, so that no color gradients are evident outside the nucleus (this color uniformity is evident by the nearly uniform whiteness of the central structures in the color composite in Fig. 1), (b) the center of the bulge isophotes for different NIR bands are coincident at the center of the optical disk, (c) the primary position angle of the bulge, about 50° , is about 10° higher than the PA of the outer disk, and (d) the boxiness of M31's bulge rivals that seen in any galaxy.

4. DISCUSSION

This new large scale infrared mapping of M31 vividly highlights the morphology of its bulge, definitively confirms earlier suggestions from optical studies (§1) of a boxy inner structure, and permits high S/N measurements of bulge shape without interference from variable dust extinction (Fig. 3). M31 clearly twins the Milky Way (Hauser et al. 1990, Weiland et al. 1994) — as well as a large fraction (45%, according to Lütticke et al. 2000) of other highly inclined disk galaxies — in having a boxy inner structure that is made more evident by infrared imaging. Indeed, K band images by Shaw (1993) and Bureau et al. (2006) of nearly 30 edge-on systems with a boxy/peanut bulge all display residual maps with Maltese cross patterns closely resembling that observed here in M31, and, when sufficiently face-on, isophotal twists. Boxy bulges are now recognized from N -body simulations to represent the vertical structure of bars viewed at high inclination (Combes et al. 1990; see review by Athanassoula 2005). This is clearly demonstrated by the Milky Way, which appears to have a boxy bulge similar to the one we observe in M31 (Binney, Gerhard & Spergel 1997, Bissantz & Gerhard 2002). The M31 inner structure can also be reproduced by self-consistent N -body modeling of a barred galaxy, as long as a classical bulge is also present (Athanassoula & Beaton 2006, see inset to Fig. 1). In this model, the bar creates and extends well past the $700''$ boxy bulge, and may even account for the $50'$ radius “pseudo-ring” of M31. The 6x images show clear evidence for this “thin bar” extending to at least $\sim 1200''$ (4 kpc). From the presence of this feature, together with the successful modeling of the images presented here using a bar potential as well as the numerous other examples of models and data indicating the close connection between bars and boxy bulges, it may be safely concluded that M31 is a barred spiral galaxy.

This publication makes use of data products from the Two Micron All Sky Survey, which is a joint project of the University of Massachusetts and the Infrared Processing and Analysis Center/California Institute of Technology, funded by the National Aeronautics and Space Administration and the National Science Foundation (NSF). We appreciate support by NSF grant AST-0307851 and a Space Interferometry Mission Key Project grant, NASA/JPL contract 1228235. RLB was supported by a Harrison Undergraduate Research Award from the University of Virginia Center for Undergraduate Research. MFS acknowledges support from NASA/JPL contract 1234021. This work was also supported by the F.H. Levinson Fund of the Peninsular Community Foundation. P.G. was supported by NSF grants AST-0307966 and AST-0507483 and NASA/STScI grants GO-10265.02 and GO-10134.02.

REFERENCES

- Athanassoula, E. 2005, MNRAS, 358, 1477
Athanassoula, E., & Beaton, R. L. 2006, MNRAS, submitted
Berman, S. 2001, A&A, 371, 476
Berman, S., & Loinard, L. 2002, MNRAS, 336, 477
Binney, J., Gerhard, O., & Spergel, D. 1997, MNRAS, 288, 365
Bissantz, N., & Gerhard, O. 2002, MNRAS, 330, 591
Blitz, L., Binney, J., Lo, K. Y., Bally, J., & Ho, P. T. P. 1993, Nature, 361, 417
Bureau, M., Aronica, G., Athanassoula, E., Dettmar, R.-J., Bosma, A., Freeman, K. C. 2006, MNRAS, in press

- Cole, A. A., & Weinberg, M. D. 2002, *ApJ*, 574, L43
- Combes, F., Debbasch, F., Friedli, D., & Pfenniger, D. 1990, *A&A*, 233, 82
- Dressler, A., & Richstone, D. O. 1988, *ApJ*, 324, 701
- Gerhard, O. E. 1988, *MNRAS*, 232, 13P
- Hackwell, J. A., & Schweizer, F. 1983, *ApJ*, 265, 643
- Hauser, M. G., et al. 1990, NASA photograph G90-03046
- Jedrzejewski, R. I. 1987, *MNRAS*, 226, 747
- Kent, S. M. 1983, *ApJ*, 266, 562
- Kormendy, J. 1988, *ApJ*, 325, 128
- Lindblad, B. 1956, *Stockholms Observatoriums Annaler*, 2,
- Light, E. S., Danielson, R. E., & Schwarzschild, M. 1974, *ApJ*, 194, 257
- Lütticke, R., Dettmar, R.-J., & Pohlen, M. 2000, *A&A*, 362, 435
- Majewski, S. R., Hereld, M., Koo, D. C., Illingworth, G. D., & Heckman, T. M. 1993, *ApJ*, 402, 125
- Newberg, H. J., & Yanny, B. 2004, *BAAS*, 205, 142.04
- Parker, J. E., Humphreys, R. M., & Larsen, J. A. 2003, *AJ*, 126, 1346
- Parker, J. E., Humphreys, R. M., & Beers, T. C. 2004, *AJ*, 127, 1567
- Quillen, A. C., Kuchinski, L. E., Frogel, J. A., & Depoy, D. L. 1997, *ApJ*, 481, 179
- Scoville, N. Z., Matthews, K., Carico, D. P., & Sanders, D. B. 1988, *ApJ*, 327, L61
- Shaw, M. 1993, *MNRAS*, 261, 718
- Skrutskie, M. F., Reber, T. J., Murphy, N. W., & Weinberg, M. D. 2001, *BAAS*, 33, 1437
- Stark, A. A. 1977, *ApJ*, 213, 368
- Stark, A. A., & Binney, J. 1994, *ApJ*, 426, L31
- Telesco, C. M., Joy, M., Dietz, K., Decher, R., & Campins, H. 1991, *ApJ*, 369, 135
- Thilker, D. A., et al. 2005, *ApJ*, 619, L67
- Weiland, J. L., et al. 1994, *ApJ*, 425, L81
- Weinberg, M. D. 1992, *ApJ*, 384, 81